H_2 Emission from the Inner 400 Parsecs of the Galaxy II. The UV–Excited H_2

Soojong Pak[1], D. T. Jaffe, and L. D. Keller[1]

Astronomy Department, University of Texas, Austin, TX 78712

Abstract. We have observed near–IR H_2 line emission on large scales in the Galactic center. Paper I discussed our 400 pc long strip map and 50 pc map of the H_2 $v = 1 \to 0$ $S(1)$ line. In this paper, we present observations of the higher vibrational lines (H_2 $v = 2 \to 1$ $S(1)$ and $v = 3 \to 2$ $S(3)$) at selected positions and conclude that strong far–UV radiations excites the H_2. We compare the H_2 $v = 1 \to 0$ $S(1)$ emission to far–IR continuum emission and show that the ratio of these two quantities in the Galactic center equals the ratio seen in the starburst galaxies, M82 and NGC 253, and in ultraluminous infrared bright galaxies.

1. Introduction

The central kpc regions in starburst galaxies and ultraluminous IR bright galaxies are powerful emitters of near-IR H_2 emission (Puxley, Hawarden, & Mountain 1990; Goldader et al. 1995). Ro–vibrational lines of H_2 can trace both photon–dominated regions (PDRs), where far–UV photons excite the H_2, and shocked regions, where the H_2 is thermally excited. Vigorous star formation in these galaxies produces large numbers of UV photons which fluorescently excite H_2, while subsequent supernovae shock–excite the H_2.

We have used the University of Texas near–IR Fabry–Perot Spectrometer, to survey giant molecular clouds (GMCs) on $1 - 10$ pc scales (Luhman et at. 1994; Luhman & Jaffe 1996; Luhman et al. 1996). In Orion A, for example, the H_2 $v = 1 \to 0$ $S(1)$ line emission extends up to 8 pc (1°) from the central UV source, θ^1 Ori C. The detection of higher vibrational state H_2 lines, e.g., $v = 6 \to 4$ $Q(1)$ and $v = 2 \to 1$ $S(1)$, showed that far–UV photons excite the H_2. Although the shock–excited H_2 emission is intense in the Orion $BN - KL$ region, the emission region is relatively compact ($\sim 1'$). The total H_2 luminosity in the $BN - KL$ region is only $\sim 1\%$ of the Orion PDR H_2 luminosity. Similarly, UV–excited H_2 dominates the large–scale H_2 emission from other GMCs.

We have observed the H_2 emission in the inner $\sim$ 400 pc ($\sim 3°$) of our Galaxy in order to investigate H_2 emission on a more global scale and to compare the Galactic center with central $\sim$ 1 kpc regions in external galaxies. The

[1]Visiting Astronomer, Cerro Tololo Inter-American Observatory, National Optical Astronomy Observatory, which are operated by the Association of Universities for Research in Astronomy, under contract with the National Science Foundation

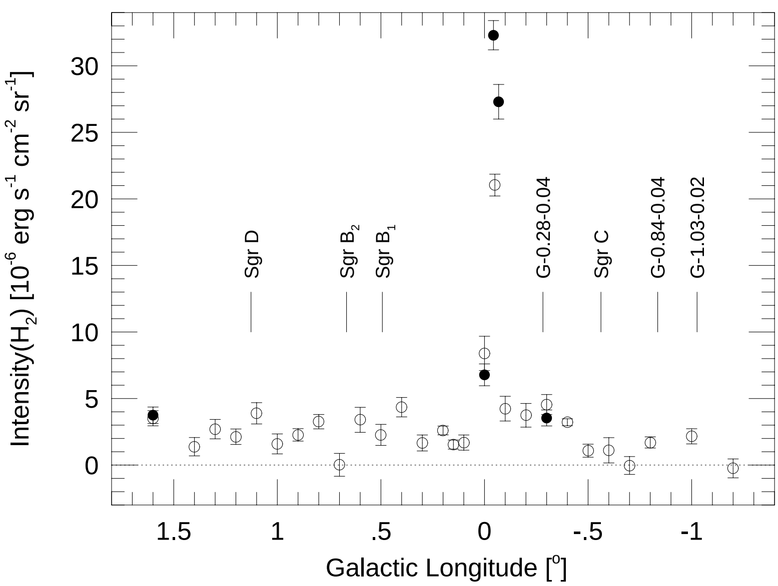

Figure 1. Observed intensity distribution of H_2 $v = 1 \rightarrow 0$ $S(1)$ ($\lambda = 2.121$ μm) along the Galactic plane at $b = -0\overset{\circ}{.}05$. The open circles were taken at the McDonald 0.9 m telescope with a $3\overset{\prime}{.}3$ beam (Paper I) and the filled circles at the CTIO 1.5 m telescope with a $1\overset{\prime}{.}35$ beam. The intensities have not been corrected for interstellar extinction. The error bars represent 1σ measurement uncertainties.

physical conditions in the interstellar medium of the Galactic center are significantly different from those in the solar neighborhood. The thin disk (diameter of 450 pc, height of 40 pc) of dense interstellar material in the Galactic center contains M(H_2) $> 2 \times 10^7 M_{\odot}$ (Güsten 1989; Hasegawa et al. 1996). The molecular clouds in the Galactic center have higher density, higher metallicity, and higher internal velocity dispersion than the clouds in the solar neighborhood (Blitz et al. 1993). There is strong radio continuum radiation from giant H II regions (Sgr A, Sgr B, Sgr C, and Sgr D) and extended low–density (ELD) ionized gas. The spectral index in the areas away from the discrete H II regions shows that thermal bremsstrahlung from ionized gas can account for about half of the emission from the extended gas (Sofue 1985). Another indicator of the intense UV radiation in the central 400 pc is strong far–IR continuum emission (Odenwald & Fazio 1984). About 90% of the far–UV energy is absorbed by dust and reradiated in the far–IR. From the far–IR intensity, we estimate that the far–UV radiation field is $\sim 10^3$ times the value in the solar neighborhood ($I_{\circ} = 4 \times 10^{-4}$ ergs s^{-1} cm $^{-2}$ sr^{-1}, Draine 1978). The energetic conditions in the Galactic center mean that the center can provide a unique view of the interaction between stellar UV radiation and molecular clouds, and serve as a nearby model for the nuclei of galaxies.

In paper I (Pak, Jaffe, & Keller 1996) we showed the distribution of H_2 $v = 1 \rightarrow 0$ $S(1)$ emission along a 400 pc–long strip and in the inner 50 pc of the Galactic center. We detected H_2 emission throughout the surveyed region. The typical dereddened ($A_K = 2.5$ mag) H_2 $v = 1 \rightarrow 0$ $S(1)$ intensity, $\sim 3 \times 10^{-5}$ ergs s^{-1} sr^{-1}, is similar to the surface brightness in Galactic PDRs (Luhman & Jaffe 1996). In this Paper, we present observations of several H_2 lines, discuss the excitation mechanism, and compare the Galactic center observations to observations of other galaxies.

2. Observations and Results

We observed three H_2 emission lines: $v = 1 \rightarrow 0$ $S(1)$ ($\lambda = 2.121$ μm), $v = 2 \rightarrow 1$ $S(1)$ ($\lambda = 2.247$ μm), and $v = 3 \rightarrow 2$ $S(3)$ ($\lambda = 2.201$ μm), at the Cerro Tololo Inter–American Observatory 1.5 m telescope in 1995 July and October. We used the University of Texas Near–Infrared Fabry–Perot Spectrometer. The instrument was specially designed to observe very extended, low surface brightness objects, and has a single channel InSb detector with surface area of 1 mm to maximize the beam size (Luhman et al. 1995). The telescope ($f/30$), a collimator (effective focal length 686 mm), and a field lens (effective focal length 20mm) produce a beam diameter of $1\overset{'}{.}35$ (equivalent disk).

The Fabry–Perot interferometer operates in 94th order ($\lambda_\circ = 2.121\mu$m) with an effective finesse of 26, yielding a spectral resolution of 125 km s^{-1} (FWHM). Scans covered in 15 sequential steps, ± 300 km s^{-1} centered at $V_{LSR} \simeq 0$ km s^{-1}. In order to subtract background and telluric OH line emission, we chopped the secondary mirror to $\Delta b = +16'$ or $-16'$ at 0.5 Hz.

We observed five positions: $(l, b) = (-0\overset{\circ}{.}0433, -0\overset{\circ}{.}0462)$, $(-0\overset{\circ}{.}0683, -0\overset{\circ}{.}0462)$, $(0\overset{\circ}{.}00, -0\overset{\circ}{.}05)$, $(-0\overset{\circ}{.}30, -0\overset{\circ}{.}05)$, and $(+1\overset{\circ}{.}60, -0\overset{\circ}{.}05)$. In Figure 1, we plot the new H_2 $v = 1 \rightarrow 0$ $S(1)$ data overlaid on the data from Paper I and compare the two data sets. The $3\overset{'}{.}3$ beam of the McDonald 0.9 m telescope centered at Sgr A* ($l = -0\overset{\circ}{.}0558$, $b = -0\overset{\circ}{.}0462$) covers the whole circumnuclear gas ring (Gatley et al. 1986), while, with the $1\overset{'}{.}35$ beam of the CTIO 1.5 m telescope, we observed the $+\Delta l$ H_2 peak $(-0\overset{\circ}{.}0433, -0\overset{\circ}{.}0462)$ and the $-\Delta l$ H_2 peak $(-0\overset{\circ}{.}0683, -0\overset{\circ}{.}0462)$. The difference between the $3\overset{'}{.}3$ beam data and the $1\overset{'}{.}35$ beam data toward Sgr A is an effect of different beam sizes because the H_2 emission sources are relatively compact. In the large–scale emission beyond Sgr A, the two data sets agree to within the errors, indicating that the H_2 emission varies slowly on $1' - 3'$ scales.

3. Extinction Correction

The extinction in K–band toward the Galactic center is significant. Figure 2a shows the classification of the extinction into *foreground extinction* by material in spiral arms at $R = 4 - 8$ kpc, and *Galactic center extinction* by material in the Galactic center clouds. Catchpole, Whitelock, & Glass (1990) measured the foreground extinction as $A_K \simeq 2.5$ mag.

A discussion of the Galactic center extinction requires a different approach because individual clouds in the Galactic center are almost opaque in the near–IR ($A_K = 10 - 30$ mag for typical clouds of $D \simeq 10$ pc and $n(H_2) \simeq 10^4$ cm^{-3}). If the UV–excited H_2 emission arises on the cloud surfaces, we need only consider the effects of shadowing by other Galactic center clouds (see Figure 2b). From millimeter observations of ^{12}CO $J = 1 \rightarrow 0$ emission, we can estimate the

Figure 2. (a) Top–view schematic of the distribution of interstellar material in two foreground spiral arms (foreground extinction) and in the GMCs in the inner ~ 400 pc of the Galaxy (Galactic center extinction). (b) Schematic diagram of small and large beam observations in the Galactic center. ^{12}CO $J = 1 \rightarrow 0$ spectrum of a typical cloud is beam diluted. The velocity–integrated intensity including the clouds in the beam at other velocities is ~ 1500 K km s^{-1}, which indicates that the area filling factor, f, is ~ 1. The cloud components do not usually overlap along the line–of–sight.

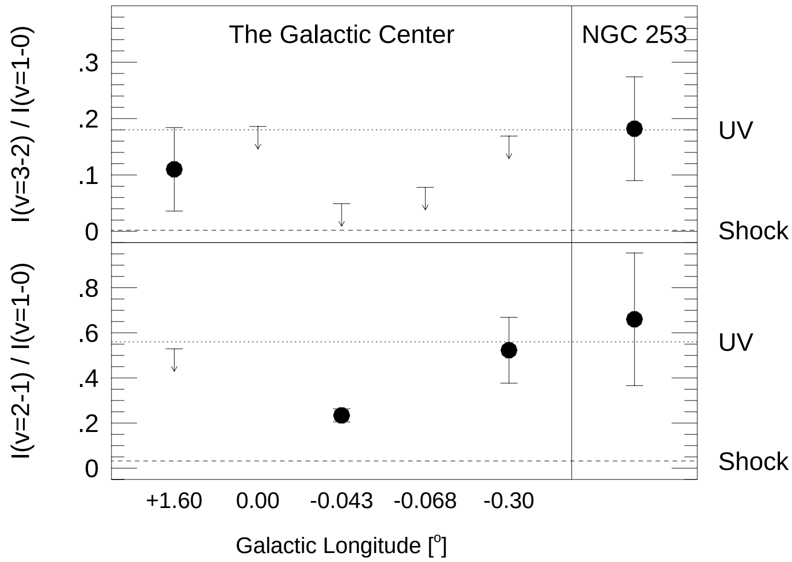

Figure 3. Observed H_2 line ratios at positions along the Galactic Plane ($b = -0\overset{\circ}{.}05$) and in the central 1 kpc of NGC 253. The dotted lines are modeled ratios of UV–excited H_2 lines, (Black & van Dishoeck 1987), and shock–excited H_2 lines ($V_{shock} = 30$ km s^{-1}; Draine, Roberge, & Dalgarno 1983). The arrows show the 3σ limits where we did not detect the higher vibrational level lines.

velocity–integrated area filling factor of clouds, f. If the millimeter telescope beam size is smaller than the individual clouds and covers only one cloud along the line–of–sight, the area filling factor, f, is 1. The upper diagram in Figure 2b shows an expected ^{12}CO $J = 1 \rightarrow 0$ spectrum of typical clouds in the Galactic center which have kinetic temperature of $\sim$ 70 K and line widths of $\sim$ 20 km s^{-1} (Güsten 1989). In general, the clouds have different sizes and may overlap along the line–of–sight. The lower diagram in Figure 2b shows an observed typical ^{12}CO $J = 1 \rightarrow 0$ spectrum where the velocity–integrated intensity is $\sim$ 1500 K km s^{-1} (Bally et al. 1987; Bally et al. 1988). The value f is the ratio of the observed velocity–integrated intensity of ^{12}CO $J = 1 \rightarrow 0$ to the single typical cloud intensity (70 K $\times$ 20 km s^{-1}). The f toward the Galactic center clouds is $\sim$ 1, implying that there is little or no overlap along a typical line–of–sight. If $f \leq 1$, we only miss the near–IR H_2 flux from the back sides of the clouds. If $f > 1$, H_2 radiation is blocked by the foreground clouds, and the ratio of the observed H_2 flux to the emitted flux is inversely proportional to f. Since $f \simeq 1$, we use the foreground values, $A_K = 2.5$, for the extinction correction.

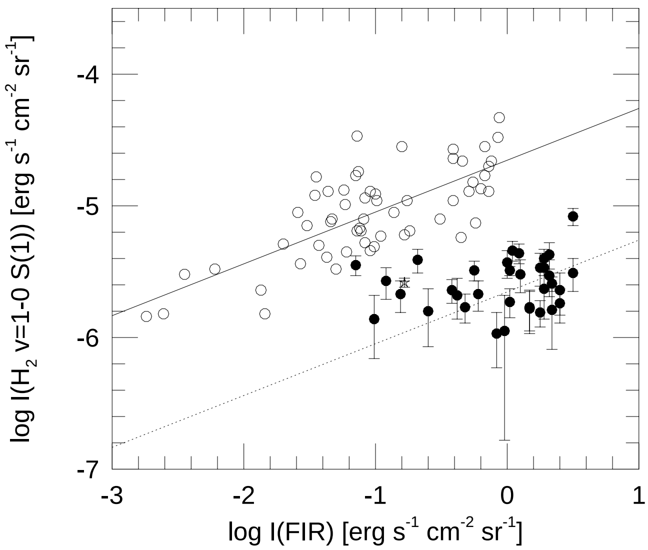

Figure 4. I_{FIR} versus $I_{H2v=1\to0\ S(1)}$ for the Galactic PDRs and the Galactic center. The open circles are from Orion A and B, ρ Ophiuchi, and G236+39 (Luhman & Jaffe 1996), and the filled circles are from the Galactic center (Paper I). The Galactic center data are not corrected for extinction. The solid line ($\log I_{H2\ v=1\to0\ S(1)} = -4.65 + 0.39 \log I_{FIR}$) is derived from the Galactic PDR data using a least squares method, and the dotted line shows the vertically shifted solid line by $\Delta \log I_{H2} = -1$.

4. H_2 Excitation Mechanism

4.1. H_2 Line Ratios

In UV–excited H_2, the branching ratios in the downward cascade determine the relative strengths of the near–IR lines. On the other hand, the energy level populations of shock–excited H_2 are thermalized. We use the line intensity ratios of higher vibrational level lines to the $v = 1 \to 0$ $S(1)$ line in order to identify the H_2 excitation mechanism.

In Figure 3, the observed ratios in the large–scale Galactic center and the central 1 kpc region of NGC 253 imply that the H_2 emission may result from UV–excitation. In the circumnuclear gas ring ($l = -0\overset{\circ}{.}0433$ and $-0\overset{\circ}{.}0683$), the UV–excited H_2 energy levels are partially thermalized because of the relatively high density (Sternberg & Dalgarno 1989; see also Ramsay-Howat, Mountain, & Geballe 1996 for the H_2 observations in the circumnuclear gas ring). The determination of line ratios consistent with UV excitation in the large–scale Galactic center and NGC 253 means the gas is not dense enough for collisions to significantly alter the radiative cascade, $n(H_2) < 10^5$ cm^{-3} (Luhman et al. 1996).

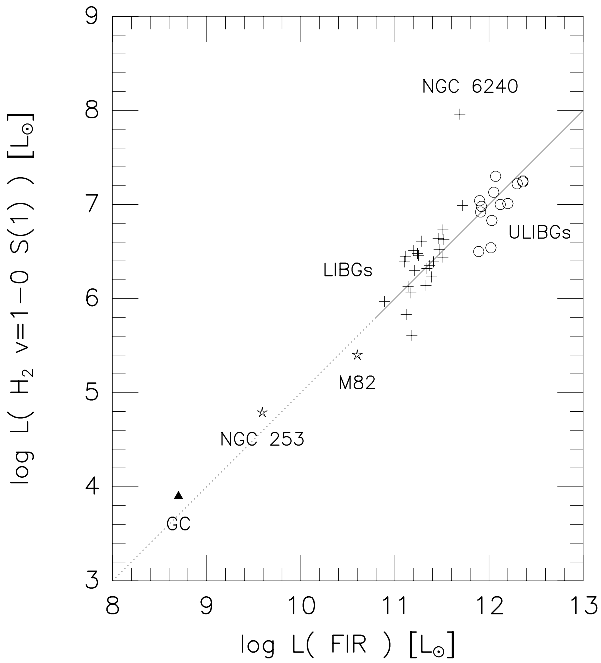

Figure 5. L_{FIR} versus $L_{H2\ v=1\rightarrow 0\ S(1)}$ of various kinds of galaxies. The solid line ($\log L_{H2\ v=1\rightarrow 0\ S(1)} = -5 + \log L_{FIR}$) is derived from data of ultraluminous IR bright galaxies (open circles) and luminous IR bright galaxies (plus signs, Goldader et al. 1995) The dotted line shows extrapolation from the solid line. The H_2 data of M82 were taken at the McDonald 2.7 m telescope and the H_2 data of NGC 253 at the CTIO 1.5 m telescope, both with the UT FPS.

4.2. I_{FIR} versus I_{H2}

If large–scale H_2 emission arises in the surface layers of the clouds where far–UV photons can excite the molecules, the dust, which absorbs the bulk of the incident flux, ought to radiate in the far–IR continuum as well. If we de–redden the Galactic center H_2 observations by $A_K = 2.5$ mag, the Galactic center results are consistent with the empirical far–IR vs. H_2 relationship derived for the UV–excited surfaces of clouds in the galactic disk (see Figure 4).

5. Comparison with other Galaxies

We extrapolate from our 400 pc long strip to the total H_2 $v = 1 \rightarrow 0$ $S(1)$ luminosity of the Galactic Center by assuming that the scale height of the H_2 emission equals that of the far–IR radiation ($h \simeq 0\overset{\circ}{.}2$, Odenwald & Fazio 1984) and that $A_K = 2.5$ mag and $f \simeq 1$. The H_2 $v = 1 \rightarrow 0$ $S(1)$ luminosity in the inner 400 pc diameter of the Galaxy is 8.0×10^3 $L_{\odot}$.

For ultraluminous and luminous infrared bright galaxies ($L_{IR} \gtrsim 10^{11}$ $L_{\odot}$), Goldader et al. (1995) showed the correlation between L_{FIR} and $L_{H2\ v=1\rightarrow 0\ S(1)}$.

We can extend the relationship to nearby starburst galaxies like M82 and NGC 253, and to the Galactic center (see Figure 5). The strong correlation between the far-IR and H_2 luminosity for various classes of galaxies indicates that the far–UV radiation may excite large scale H_2 emission in all of these sources.

Acknowledgments. This work was supported by NSF grant AST 9117373 and by David and Lucile Packard Foundation. We thank M. Luhman and T. Benedict for contributions to the Fabry–Perot Spectrometer Project, and J. Elias, B. Gregory, and the staff of the CTIO for their assistance in setting up our instrument.

References

Bally, J., Stark, A. A., Wilson, R. W., & Henkel, C. 1987, ApJS, 65, 13

Bally, J., Stark, A. A., Wilson, R. W., & Henkel, C. 1988, ApJ, 324, 223

Black, J. H., & van Dishoeck, E. F. 1987, ApJ, 322, 412

Blitz, L., Binney, J., Lo, K. Y., Bally, J., Ho, P. T. P. 1993, Nature, 361, 417

Catchpole, R. M., Whitelock, P. A., & Glass, I. S. 1990, MNRAS, 247, 479

Draine, B.T. 1978, ApJS, 36, 595

Draine, B. T., Roberge, W. G., & Dalgarno, A. 1983, ApJ, 264, 485

Gatley, I., Jones, T. J., Hyland, A. R., Wade, R., Geballe, T. R., & Krisciunas, K. 1986, MNRAS, 222, 299

Goldader, J. D., Joseph, R. D., Doyon, R., & Sanders, D. B. 1995, ApJ, 444, 97

Güsten, R. 1989, in IAU Symp. 136, The Center of the Galaxy, ed. M. Morris (Dordrecht: Kluwer), 89

Hasegawa, T., Oka, T., Handa, T., Hayashi, M., & Sakamoto, S. 1996, this volume

Luhman, M.L., & Jaffe, D.T. 1996, ApJ, 483(May 20 issue)

Luhman, M. L., Jaffe, D. T., Keller, L. D., & Pak, S. 1994, ApJ, 436, L185

Luhman, M. L., Jaffe, D. T., Keller, L. D., & Pak, S. 1995, PASP, 107, 184

Luhman, M. L., Jaffe, D. T., Sternberg, A., Herrmann, F., & Poglitsch, A. 1996, ApJ, in preparation

Odenwald, S. F., & Fazio, G. G. 1984, ApJ, 283, 601

Pak, S., Jaffe, D. T., & Keller, L. D. 1996, ApJ, 457, L43 (Paper I)

Puxley, P. J., Hawarden, T. G., & Mountain, C. M. 1990 ApJ, 364, 77

Ramsay-Howat, S., Mountain, C. M., & Geballe, T. R. 1996, this volume

Sofue, Y. 1985, PASJ, 37, 697

Sternberg, A., & Dalgarno, A. 1989, ApJ, 338, 197